absorption and emission[11]; the position-dependence of the band edge for majority carriers with respect to the Fermi level, from position-dependent conductivity and the photovoltaic effect.[12]

Hill and Williams[13] have reported electric-field-dependent luminescence spectra in graded zinc-cadmium sulfide crystals. They have interpreted the linear shift in the edge emission spectrum as field-enhanced minority-carrier transport between regions of different band gaps. Shifts up to 45 Å for band-gap gradients of a few eV/cm were obtained with applied fields of the order of 10^4 V/cm. Solutions of Eq. (16) can be used to determine theoretically the field dependence of emission spectra. Also, the density of states affects the field dependence. From the inequalities (5), it is apparent that much larger shifts can be predicted for mixed semiconductors with larger composition gradients.

Electroluminescence could in principle be achieved by a mechanism specific to graded-band-gap systems, a region of which has a near-zero band gap. Minority carriers thermally generated in the small-gap region would be transported to a region of larger gap by an applied electric field, followed by radiative recombination.[14]

Finally, we propose that the behavior of excitons in graded mixed semiconductors be investigated. For proper systems, the valence and conduction-band gradients can induce motion in the same direction for both electrons and holes. Thus graded-gap systems have unique advantages for the study of exciton transport.

ACKNOWLEDGMENTS

[11] L. J. Van Ruyven and I. Dev, J. Appl. Phys. 37, 3324 (1966).
[12] Indradev, L. J. Van Ruyven, and F. Williams, J. Appl. Phys. 39, 3344 (1968).
[13] R. Hill and F. Williams, Appl. Phys. Letters 11, 296 (1967).

[14] F. Williams, in *II–VI Semiconducting Compounds* (W. A. Benjamin, Inc., New York, 1967), p. 1476.

Radiative Spectra from Shallow Donor-Acceptor Electron Transfer in Silicon*

R. C. ENCK† AND A. HONIG

Syracuse University, Sycrause, New York 13210

(Received 22 July 1968)

Radiation associated with shallow donor-acceptor electron transfer in silicon has been examined in the liquid-helium temperature region for various combinations of group-V donors and group-III acceptors. The spectra for all impurities are quite similar, exhibiting TA- and TO-phonon–assisted lines, as well as a no-phonon line in all but the (Sb,B)-doped sample. A (P,In) sample exhibits an unusual extra line which is attributed to an LA-phonon–assisted transition. A theory analogous to that of Thomas, Hopfield, and Augustyniak, modified to take account of anisotropic donor wave functions, is used to analyze the line shapes and determine rate constants and the impurity-pair Coulomb energy for pairs that decay at different times after impurity neutralization. This leads to a direct measurement of the indirect silicon energy gap of 1.166 ±0.0010 eV and an exciton binding energy of 0.0102±0.0015 eV, when combined with infrared-absorption measurements near the indirect gap. The analysis also indicates that optically determined impurity ionization energies are correct, and that the thermally determined impurity activation energies and their concentration dependence probably result from carrier redistribution effects rather than modification of the impurity ionization energies of the majority of the impurities.

1. INTRODUCTION

RADIATIVE spectra and recombination kinetics associated with electron transfer between shallow donors and acceptors have been reported for several

[1] J. J. Hopfield, D. G. Thomas, and M. Gershenzon, Phys. Rev. Letters 10, 162 (1963).
[2] D. G. Thomas, J. J. Hopfield, and K. Colbow, in *Proceedings of the Symposium on Radiative Recombination in Semiconductors* (Dunod Cie., Paris, 1965), p. 67.
[3] K. Colbow, Phys. Rev. 139, A274 (1965).
[4] D. G. Thomas, J. J. Hopfield, and W. M. Augustyniak, Phys. Rev. 140, A202 (1965).
[5] C. Benoit à la Guillaume and J. Cernogora, in *Proceedings of*

semiconductors, among which the most studied are GaP,[1–4] germanium,[5,6] and silicon.[7–10] The luminescence

the Symposium on Radiative Recombination in Semiconductors (Dunod Cie., Paris, 1965), p. 121.
[6] V. P. Dobrego, S. M. Ryvkin, and I. S. Shlimak, Fiz. Tverd. Tela 8, 2124 (1966); 9, 1451 (1967) [English transls.: Soviet Phys.—Solid State 8, 1689 (1967); 9, 1131 (1967)].
[7] A. Honig, in *Proceedings of the International Conference on Semiconductor Physics, Prague, 1960* (Academic Press Inc., New York, 1961), p. 610.
[8] A. Honig and R. Enck, in *Proceedings of the Symposium on Radiative Recombination in Semiconductors* (Dunod Cie., Paris, 1965), p. 113.
[9] Ya. E. Pokrovskii and K. I. Svistunova, Fiz. Tverd. Tela 7, 1837 (1965) [English transl.: Soviet Phys.—Solid State 7, 1478 (1965)].
[10] V. S. Vavilov, O. G. Koshelev, Yu. P. Koval', and Ya. G. Klyava, Fiz. Tverd. Tela 8, 3449 (1966) [English transl.: Soviet Phys.—Solid State 8, 2770 (1967)].

associated with this type of recombination process can consist of discrete lines or a continuous band, and may or may not be assisted by momentum-conserving phonons, depending on the band structure and the nature of the impurities. Aspects of this problem which have been studied include the competition between donor-acceptor and band-impurity recombination[9] and the use of electron paramagnetic resonance (EPR) to measure transition rates.[7,8,10] A recent review article on the general topic of donor-acceptor recombination discusses most of the areas of current interest in this field.[11]

In a previous work on shallow donor-acceptor recombination radiation in silicon,[8] the radiative spectra for various impurities were reported, and it was suggested how further analysis of this process could provide accurate information concerning the indirect energy gap in silicon, impurity and exciton binding energies, and phonon selection rules. That work has been extended to include most of the shallow impurities in silicon and a wide range of decay times, and an analysis has been carried out which does yield the above-cited information.

In this paper, we first describe the experimental methods used to observe recombination radiation spectra as a function of time after the electric charges of the donors and acceptors are optically neutralized. An analysis of line separation in these spectra gives selection rules and energies of phonons involved in indirect transitions, while comparison of theoretical and experimental line shapes as a function of delay time after neutralization permits the determination of the recombination rate constants and the separations of the donor-acceptor pairs which contribute to the radiation peaks at different times. This leads to a determination of the energy gap and the exciton binding energy, as well as to better understanding of the impurity ionization energies.

2. EXPERIMENTAL CONSIDERATIONS

The samples used in this study were cut from compensated n-type single crystals of silicon and etched. Their sizes were approximately $4\times5\times3$ mm. The impurity concentrations were obtained from two types of measurement. Room-temperature resistivity measurements gave directly the difference between the donor concentration N_D and the acceptor concentration N_A, and liquid-helium-temperature EPR measurements in the equilibrium charge-state condition and in the metastable condition, where most impurities are neutral as a consequence of intrinsic illumination, yielded[12] $(N_D-N_A)/N_D$. From N_D-N_A and $(N_D-N_A)/N_D$ both N_D and N_A are determined. Concentration values so determined were checked in several samples by Hall measurements and gave satisfactory agreement. The

[11] F. Williams, Phys. Status Solidi **25**, 493 (1968).
[12] A. Honig, in *Quantum Electronics*, edited by C. H. Thomas (Columbia University Press, New York, 1960), p. 450.
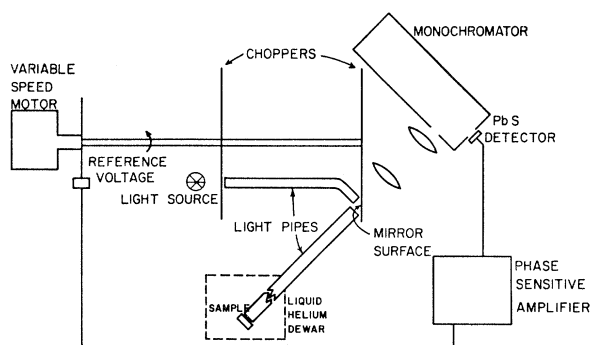
FIG. 1. Schematic diagram of experimental apparatus.

samples and their impurity concentrations are listed in Table I.

The experiments described in this paper were performed with the apparatus shown schematically in Fig. 1. The two choppers have five evenly spaced teeth and are mounted on a common shaft. The chopper nearest the light source has open sectors of 30°, while the other one has open sectors of 10° and a mirror finish on the side toward the light pipe. The midpoints of both open sectors are arranged to be 36° apart. The shaft is driven by a synchronous motor through a 10-speed gearbox (Insco Corp.).

When the light source, a 150-W projection lamp with an internal focusing mirror, is uncovered by the first chopper, pumping light is transmitted through the first (rigid) light pipe, reflected from the mirror surface of the second chopper, and transmitted through the second (incoherent, flexible) light pipe. It then strikes the sample, which is butted up against the end of the light pipe, creating free holes and electrons which rapidly neutralize the shallow impurities. As the choppers rotate, the pumping light is cut off by the first chopper, and after a time delay, the second chopper allows the recombination radiation from the sample to pass from the light pipe to the monochromoter. The time delay from the cutoff of the pumping radiation to the center of the recombination radiation pulse is $0.236T$, where T is one period. Since the open sector of the second chopper transmits for only a small fraction of a

TABLE I. Silicon samples used in this study.

Silicon samples (donors, acceptors)	N_D Donor conc. (cm^{-3})	N_A Acceptor conc. (cm^{-3})
(P,B)	6.0×10^{16}	3.0×10^{16}
(P,Al)	1.5×10^{16}	3.6×10^{15}
(P,Ga)	2.8×10^{16}	2.4×10^{16}
(P,In)	5.0×10^{16}	3.0×10^{16}
(Sb,B)	5.9×10^{16}	1.7×10^{16}
(As,B)	3.4×10^{16}	1.2×10^{16}
(Bi,B)	$\sim2\ \times10^{16}$ [a]	$\sim4\ \times10^{15}$ [a]
(P,B)I	6.0×10^{15}	2.0×10^{15}
(P,B)II	1.8×10^{17}	1.8×10^{15}

[a] Because of a strong gradient of donor concentration in the bismuth-doped sample, it was not possible to make an accurate determination of N_D and N_A.

period, this mean time was taken as the delay time in the measurement. This gives the following delay times between the end of sample irradiation and the measurement of recombination radiation for the chopper rates used:

$150\,\mathrm{Hz}\rightarrow 1.57\times10^{-3}\,\mathrm{sec}$, $\quad 9.375\,\mathrm{Hz}\rightarrow 2.52\times10^{-2}\,\mathrm{sec}$,

$37.5\,\mathrm{Hz}\rightarrow 6.29\times10^{-3}\,\mathrm{sec}$, $\quad 2.344\,\mathrm{Hz}\rightarrow 1.01\times10^{-1}\,\mathrm{sec}$.

The primary reason for using fiber optics instead of conventional optics was the unavailability of a suitable optical Dewar. There were, however, other benefits inherent in this system, in particular the large $f/0.5$ aperture of the fiber optics and the great light-gathering power of the internal mirror of the 150-W projection lamp. These combined to give an extremely efficient optical pumping system. Since the 1.2-m fiber-optics light pipe stops transmitting at $\lambda \gtrsim 1.7\,\mu\mathrm{m}$, it also filters out most of the extrinsic radiation.

The Bausch and Lomb 500-mm monochromator has a grating blazed for 5000 Å in the first order. A wavelength marker and a linear wavelength drive were incorporated, and a 1-mm slit width (3.3-nm bandwidth) was used unless otherwise specified. The detector was a PbS photoconductor operated at $-80°C$, and the output of the phase-sensitive amplifier was displayed on a strip chart recorder. The coordinates of a smooth curve through the experimental spectra were then processed by a computer which corrected for the monochromator transmission, converted wavelength intervals to energy intervals, normalized the curves, and plotted the results.

We attempted to make transient measurements at shorter times than were possible with the system described above by using either a xenon flash tube or a cooled ytterbium-in-glass pulsed laser with a 1.02-$\mu\mathrm{m}$ emission as pumping sources and a cooled photomultiplier tube with an S-1 cathode as the detector. These experiments were not very successful, primarily because of the very low sensitivity of the photomultiplier tube in our wavelength region. In addition, the xenon flash tube had a relatively low-energy output and the laser exhibited a long pulse length.

In all of these experiments the sample was immersed in liquid helium (or liquid hydrogen) and temperature variation was achieved by pumping on the liquid. Helium bubbling above the λ point caused no trouble because of the good contact between the sample and the end of the flexible light pipe. Care was taken to shield the sample from radiation other than that which passed through the light pipe.

3. TRANSITION RATES AND LINE SHAPE

The energy of light emission $E(R)$ which results from the recombination of a bound electron with a bound hole is given by[1,11,13]

$$E(R)=E_g-(E_A+E_D)+e^2/\epsilon R \pm E_{\mathrm{phonon}}, \qquad (1)$$

provided that the donor-acceptor separation R is large compared to the donor and acceptor Bohr radii. E_g is the indirect gap energy, E_A and E_D are the donor and acceptor ionization energies, e is the electronic charge, ϵ is the low-frequency dielectric constant, and E_{phonon} is the energy of phonons which may be absorbed or emitted in this process. The $+$ sign corresponds to phonon absorption and the $-$ sign to emission. The term $e^2/\epsilon R$ is the Coulomb energy E_{Coul} associated with the ionized donor-acceptor pair. Since silicon is an indirect-gap material, we expect phonon participation in the recombination process, with the phonon wave vector equal to k_c, the wave vector at the lowest conduction-band minimum. Since no appropriate phonons are available for absorption at liquid-helium temperatures, only the negative sign in Eq. (1) is used.

An approximate theory for an indirect-gap material[3,4] gives a radiative recombination rate $W(R)$ for a donor-acceptor pair with isotropic wave functions,

$$W(R)=W_0\exp(-2R/b), \qquad (2)$$

where W_0 is a rate constant, R is the separation of the impurities, and b is the larger of the Bohr radii of the two impurities.

Miller and Friedman[14] have proposed a form for $W(R)$ which takes into account the anisotropy of the donor wave function. It applies to the single-photon, no-phonon process in silicon when the pair separation exceeds about 50 Å:

$$W(\mathbf{R})=W_0\{\exp[(-2/a_1)(R_y{}^2+R_z{}^2+(a_1/a_2)^2R_x{}^2)^{1/2}]$$
$$\times\sin^2 k_c R_x+\exp[(-2/a_1)(R_x{}^2+R_z{}^2+(a_1/a_2)^2$$
$$\times R_y{}^2)^{1/2}]\sin^2 k_c R_y+\exp[(-2/a_1)$$
$$\times(R_x{}^2+R_y{}^2+(a_1/a_2)^2R_z{}^2)^{1/2}]\sin^2 k_c R_z\}, \qquad (3)$$

where $\mathbf{R}=(R_x\hat{\imath},R_y\hat{\jmath},R_z\hat{k})$ is the vector joining donor impurity to acceptor impurity, a_1 is the transverse donor radius, a_2 is the longitudinal donor radius, and k_c is the magnitude of the wave vector at the conduction-band minimum. W_0 is a constant defined by

$$W_0=\frac{4^8}{9}\frac{\pi^2e^2\bar{n}}{m^2c^3}\frac{E_s|A|^2|c^{(1)}|^2(d^{(1)}-d^{(2)})^2}{a_2 a_1{}^2 a^2 k_c{}^8 r_1{}^5}, \qquad (4)$$

where c is the velocity of light, m is the free-electron mass, $\bar{n}$ is the index of refraction, a is the lattice constant, r_1 is the acceptor-state radius, and E_s is the energy separation between the donor state and the acceptor state. The remaining constants A, $c^{(1)}$, $d^{(1)}$, and $d^{(2)}$ are constants which appear in the donor-state wave function and acceptor-state wave function.[14] When appropriate numerical values are substituted in

---

[13] F. E. Williams, J. Phys. Chem. Solids 12, 265 (1960).
[14] A. Miller and B. Friedman (to be published).

Eq. (4), one finds

$$W_0 = 1.1 \times 10^{-43}/r_1{}^5 a_2 a_1{}^2 \text{ in cgs units.}$$

It is seen from Eqs. (3) and (4) that this theory is asymmetrical with respect to donor and acceptor radii. The donor radius appears in the exponent regardless of which radius is larger. This arises because of the oscillating nature of the donor wave function due to the conduction-band minimum at $k \neq 0$ as compared with the acceptor wave function derived from a valence-band maximum at $k = 0$.

Since $k_c |\mathbf{R}| > 50$ for the pair separations that concern us, $\sin^2(k_c R_{x,y,z})$ oscillates rapidly as a function of $|\mathbf{R}|$ and will be averaged because of the finite bandpass of the monochromator. We therefore take the average value over a cycle for these terms and rewrite Eq. (3) in spherical coordinates

$$W(\mathbf{R}) = \tfrac{1}{2} W_0 [W_1(R,\theta,\phi) + W_2(R,\theta,\phi) + W_3(R,\theta)],$$

where

$$W_1(R,\theta,\phi) = \exp\{-\rho[\sin^2\theta(1 + (\gamma - 1)\cos^2\phi) \\ + \cos^2\theta]\},$$

$$W_2(R,\theta,\phi) = \exp\{-\rho[\sin^2\theta(1 + (\gamma - 1)\sin^2\phi) \quad (5) \\ + \cos^2\theta]\},$$

$$W_3(r,\theta) = \exp\{-\rho[1 + (\gamma - 1)\cos^2\theta]\},$$

with

$$\rho = 2R/a_1 \quad \text{and} \quad \gamma = (a_1/a_2)^2.$$

Equation (5) holds for an isolated donor-acceptor pair. We proceed to derive results for a random distribution of a large number of impurities such as would be found in a real crystal. The treatment of Thomas, Hopfield, and Augustyniak[4] will be followed, but it will be generalized to the case of an anisotropic donor impurity. The assumption of a random distribution of donor-acceptor separations is probably not justified for very close pairs, but might be reasonable for the cases that we are considering, where $R > 50$ Å.[11] For such impurity separations, the discrete line spectrum which one would expect for very close pairs due to the restriction of impurities to lattice sites is smeared into a continuous spectrum[2,11] and the impurities can be considered as if continuously distributed.

Taking the zero of energy as $E_g - (E_D + E_A) - E_{\text{phonon}}$, Eq. (1) becomes

$$E(R) = e^2/\epsilon R. \quad (6)$$

We shall use this form for the statistical analysis.

The model which will be considered consists of a single impurity of one type (for definiteness, an acceptor) surrounded by a large number of randomly located donors. We assume that the acceptor and donors are neutral at time $t = 0$. Consider the function $\langle J_\mathbf{R}(t) \rangle$, which is analogous to $\langle J_E(t) \rangle$ in Eq. (18) of Ref. 4. $\langle J_\mathbf{R}(t) \rangle$ is emitted light intensity at time t, averaged over all donor distributions, for a donor-acceptor pair

with separation $|\mathbf{R}|$, where $|\mathbf{R}|$ is related to E through Eq. (6). $\langle J_\mathbf{R}(t) \rangle$ includes the angular dependence of the recombination rate at given $|\mathbf{R}|$. One obtains, by an analysis similar to that in Ref. 4,

$$\langle J_\mathbf{R}(t) \rangle = W(\mathbf{R}) \exp[-W(\mathbf{R})t]\langle Q(t) \rangle. \quad (7)$$

$\langle Q(t) \rangle$ is the average over all donor distributions of the probability that the acceptor has not been ionized prior to time t by any donor. In order to find the average intensity per acceptor at a given energy, we must now sum $\langle J_\mathbf{R}(t) \rangle$ over all possible angular orientations of the impurity pairs with $|\mathbf{R}|$ appropriate to the given energy, as expressed by Eq. (6). Multiplying $\langle J_\mathbf{R}(t) \rangle$ by the number of available donors $N_D R^2 dR d\Omega$ and integrating over the angular coordinates, one gets the following expression for $K_E(t)$, the intensity per acceptor per unit $|\mathbf{R}|$:

$$K_E(t) = N\langle Q(t) \rangle R^2 \int_0^\pi \int_0^{2\pi} W(R,\theta,\phi)$$

$$\times \exp[-W(R,\theta,\phi)t]\sin\theta d\phi d\theta. \quad (8)$$

This can be expressed as the sum of three integrals, each of which (under suitable rotations of coordinates) is equal to

$$(\tfrac{1}{2})N_D\langle Q(t) \rangle R^2 W_0 \int_0^\pi W_3(R,\theta) \int_0^{2\pi} \exp[-W(R,\theta,\phi)t]$$

$$\times \sin\theta d\phi d\theta. \quad (9)$$

Since a distance range $|d\mathbf{R}|$ corresponds through Eq. (6) to an energy range

$$|dE| = (e^2/\epsilon R^2)|d\mathbf{R}|, \quad (10)$$

Eq. (8) can be converted to $I(E,t)$, the intensity per acceptor per unit energy at energy E and time t

$$I(E,t) = (\tfrac{3}{2})N_D W_0 \langle Q(t) \rangle \beta^3 E^{-4} \int_0^\pi W_3(\beta E^{-1},\theta)$$

$$\times \int_0^{2\pi} \exp[-W(\beta E^{-1},\theta,\phi)t]\sin\theta d\phi d\theta, \quad (11)$$

where $\beta = e^2/\epsilon$.

Note that $I(E,t)$, the spectral line shape at a time t given by Eq. (11), is a function only of a_1, a_2, and the product $W_0 t$, and does not depend on the impurity concentration or on $\langle Q(t) \rangle$, which are merely multiplicative constants. Thus a line-shape comparison with theory may give information about the donor wave functions, as well as the rate constants. First, the applicability of the model to the real situation must be discussed further.

A difficulty with the model is that it does not take into account the presence of other acceptors. The major statistical effect of the other acceptors is random removal of electrons from some of the N_D donors. This results in changes of the number of effective donors surrounding an acceptor and in $\langle Q(t) \rangle$, which should
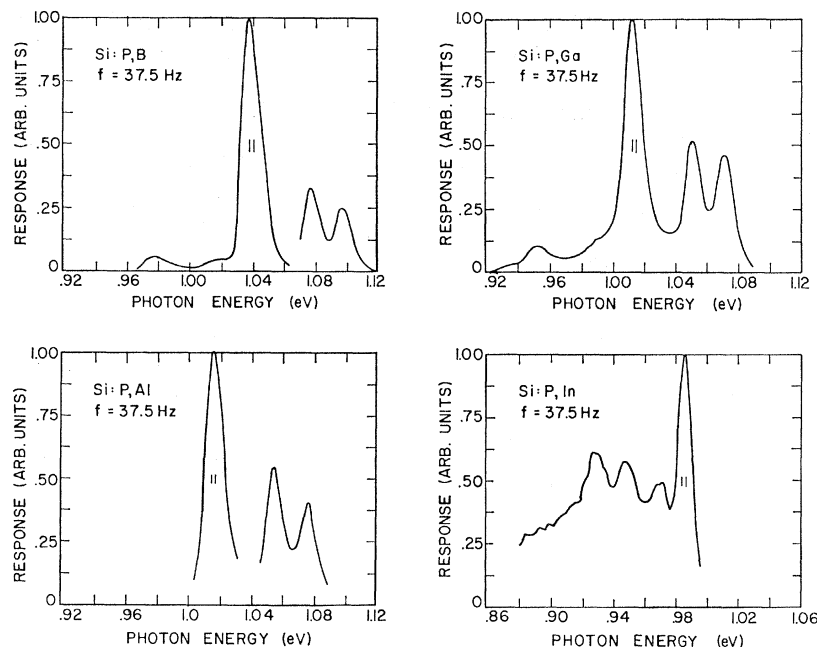
FIG. 2. Luminescence spectra of (P,B), (P,Al), (P,Ga), and (P,In) silicon samples at 37.5-Hz chopping rate. $T = 4.2$ K.

affect the relative line intensities at different times but not the line shapes. Nevertheless, an additional consideration is that these transitions to other acceptors result in charged impurities in the environment of the central acceptor and the resultant Coulomb interaction energy could cause energy shifts, especially in the higher-concentration samples. Since this process involves positive donor ions as well as negative acceptor ions, it might be expected to cause line broadening rather than line peak shifts.

Another assumption in the previous development is the neutral charge-state condition of the donors and acceptors at $t=0$ (i.e., at the time that the pumping light goes off). If the pumping light is not sufficiently intense to produce enough electron-hole pairs to neutralize all the impurities, the situation must be reexamined with this altered initial condition. If the non-neutral impurities appeared randomly, the previous assumption of a random distribution would still be valid, although the effective donor concentration surrounding an acceptor would change. This would leave the line shape unchanged while changing the relative intensities at different times. There are, however, at least two reasons to expect ionized impurities to appear nonrandomly. First, the recombination rate for donor-acceptor pairs increases rapidly for decreasing pair separation. Below a certain separation, which depends on the pumping light intensity, the electrons and holes recombine faster than they are trapped from the bands, and the impurity pairs with smaller separation than this will not be neutral at $t=0$. Second, as pointed out by Thomas, Hopfield, and Augustyniak,[4] the trapping from the bands at a particular ionized impurity might be expected to depend on the separation

of this impurity from the nearest ionized impurity of opposite sign. To see this, we consider a carrier in the conduction or valence band passing this pair of impurities with an impact parameter large compared to the interimpurity separation. The particle then sees only a dipole field due to the impurities, and the capture cross section is small. For small impact parameters, the effective field is essentially a Coulomb field and the capture cross section is large. Experiments in GaP supporting this argument have been reported.[4]

Both of these effects lead to neutralized distant pairs and charged close pairs, with the pair separation R_s, above which the impurities are saturated (neutral) determined by the pumping light intensity. Thus a saturated line should be broader than a nonsaturated one, since in the former case, the close pairs which are responsible for line broadening on the high-energy side contribute more strongly to the emitted radiation. These qualitative effects were observed and are reported in Sec. 4 D. However, a quantitative theory for the nonsaturated condition has not been formulated, and an effort was made to confine the quantitative experimentation to conditions where saturation of relevant pairs was nearly complete.

4. RESULTS AND DISCUSSION

A. Spectra and Phonons

Typical spectra taken at 4.2 K are shown in Figs. 2 and 3 for (P,B), (P,Al), (P,Ga), and (P,In) silicon samples and for (As,B), (Sb,B), and (Bi,B) silicon samples, respectively. The intensities are normalized to unity at the largest peak for a given sample, but relative intensities for different samples are not rep-

resented on the figures. The chopping rate f used in these representative spectra is 37.5 Hz for all the samples except the (Bi,B), where $f = 150$ Hz in order to improve the signal-to-noise ratio. The effects of varying chopping rate will be examined below, but we first turn our attention to more general characteristics of the spectra.

Most of the spectra for the various samples are similar, except for shifts on the energy axis. The general pattern consists of three lines of comparable magnitude and one line at the low-energy end which is an order of magnitude weaker. These lines, going from the highest-energy line progressively to lower energy, correspond to emission of a single photon with no phonon (NP), a single photon plus transverse acoustical (TA) phonon, a single photon plus transverse optical (TO) phonon, and a single photon plus two transverse optical (2TO) phonons. These identifications will be established later in this section. The shoulder seen on the low-energy wing of the TO lines (for the samples with the strongest emissions) is consistent with the emission of a photon plus one TO and one TA phonon. Some deviations from the general pattern are also apparent. For the (Sb,B) sample, the NP line is missing. The maximum amplitude that it could have is 3% of that of the TO line. The (P,In) sample exhibits an extra line between the TA and TO lines, which we attribute to a longitudinal-acoustical-phonon–assisted transition. Relative intensities of the components of the spectra vary somewhat among the different samples. Most evident among these differences is the prominence of the NP line over the TO line in the (P,In) sample. The 2TO lines are shown only for (P,B), (P,Ga), and (Sb,B) simply because these yield the strongest signals. However, weak 2TO lines have been discerned for most of the other samples, and the nonappearance of this particular weak line on some of the spectra is not meant to signify its absence or disparate small amplitude in relation to the TO line. The linewidths at a given chopping rate vary a small amount among the different samples. For a given sample, the NP lines are slightly (~ 1 meV) narrower than their phonon-assisted replicas.

Spectra similar to those of Figs. 2 and 3 were taken at different chopping rates. As one lowers the chopping rate, the linewidth becomes narrower and the line intensity weaker. The effect of chopping rate on linewidth is shown in Fig. 4 for one sample, (P,B). The linewidth dependence arises because slow chopping rates select out radiation from distant donor-acceptor pairs which are subject to smaller variation of Coulomb energy. In Sec. 4 B, this dependence is examined quantitatively and used to determine the Coulomb energy of the pairs involved in the recombination radiation. For the present, we note that narrower lines at slower chopping rates allow a more accurate determination of the energy separation of lines in the spectra and hence of the phonon energies. In addition,
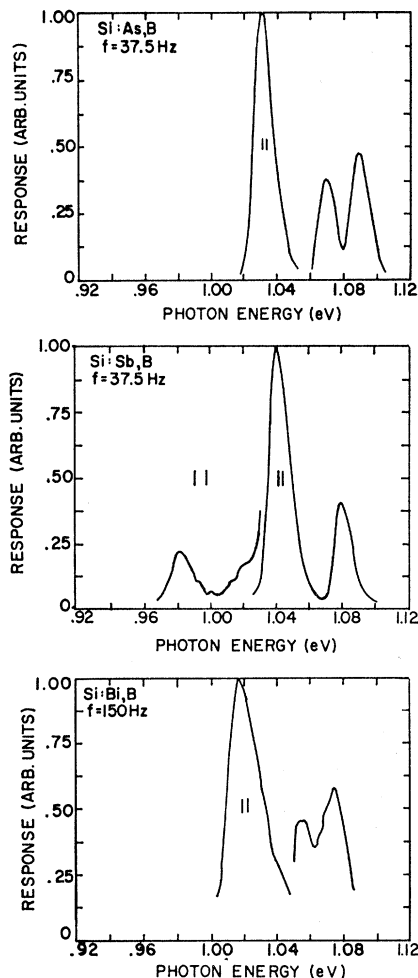

FIG. 3. Luminescence spectra of (As,B) and (Sb,B) silicon samples at 37.5-Hz chopping rate and of (Bi,B) sample at 150-Hz chopping rate. $T = 4.2$ K.

we are interested in the slower chopping rates because the pairs whose radiation is selected out are the more distant ones, and the ones most likely to be saturated, i.e., neutralized, at time $t = 0$.

As pointed out in Sec. 3, the analysis depends on all of the donors being neutral at $t = 0$. In order to check on the neutrality of the charge state (or saturation) of the impurities, we superimposed spectra taken with full pumping light intensity upon spectra taken with half pumping light intensity. If the class of pairs which is contributing to the spectrum in question (by virtue of having a decay time constant or, equivalently, a pair separation appropriate to the frequency in use) is largely neutral at $t = 0$, doubling the light intensity does not change the saturation, and the shape of the curve does not change. The absolute intensity does increase, probably because of an increase in the penetration depth, increasing the volume of the sample which is emitting. When the shape does change, it indicates that some of the pairs involved in the emission are not
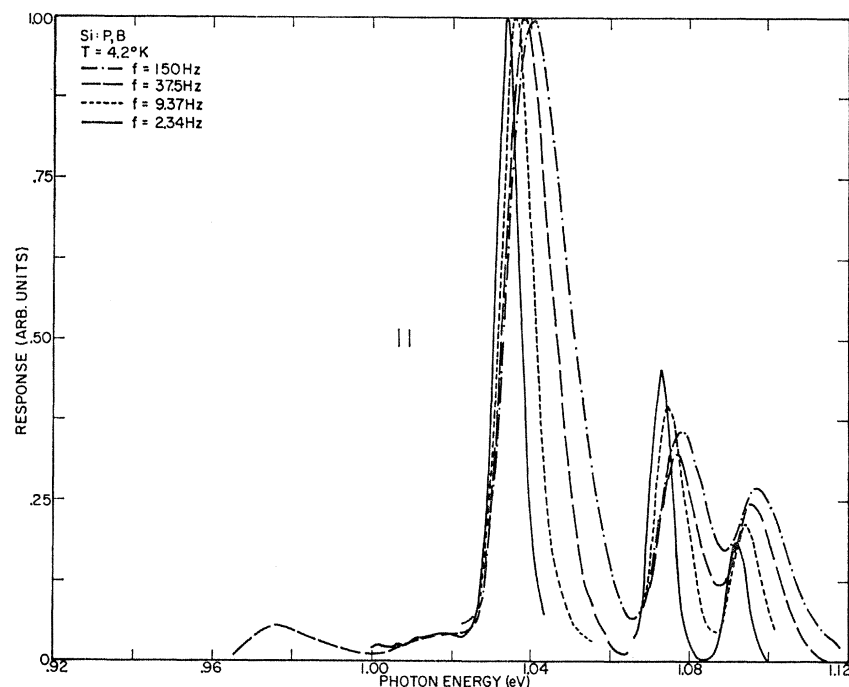
FIG. 4. Luminescence spectra of (P,B) silicon sample as a function of chopping rate. $T = 4.2$ K.

saturated and the theory does not apply to the spectra taken at this chopping rate or any faster one. Once a chopping rate is found for which the spectrum saturates, all slower rates will also give saturation. For $f = 150$ Hz, all samples were found to be unsaturated, while at $f = 9.375$ Hz, all the samples were saturated. At 37.5 Hz, most of the samples were completely saturated, and the few that were not showed only a slight lack of saturation.

The identification of the phonon-assisted lines was made from the measured line separations. One expects the separation between the NP line and the phonon replica lines to equal the energy of the appropriate phonon(s) with wave vector equal to k_c. The peak

FIG. 5. Energy separation of phonon replica peaks for silicon samples with different combinations of donors and acceptors.

separations of the lines for our samples are shown in Fig. 5 and lead to the following energies for wave-vector-conserving $(k = k_c)$ phonons:

TA phonon: 　　　　18.9±0.4 meV;

TO phonon: 　　　　58.3±0.4 meV;

$\frac{1}{2}$(2TO) phonons: 　59.8±0.4 meV.

The TA and TO phonon energies are in agreement with other wave-vector-conserving phonon energy evaluations made from infrared-absorption studies,[15] recombination-radiation experiments,[16,17] and neutron scattering experiments.[18] The larger value of $\frac{1}{2}$(2TO) may arise because of a shift in the most probable phonon wave vector from the value corresponding to the conduction-band minimum to a value corresponding to about half of the conduction-band minimum. From the neutron scattering experiments of Brockhouse,[18] it is seen that this would correspond to an increase of about 3% in phonon energy, in accord with our measurement. The above discussion was predicated on the assumption that the peaks of the NP line and the phonon-assisted lines for a given sample have equal Coulomb energies. These Coulomb energies are determined in Sec. 4 B for the NP and TO lines, and are shown indeed to have equal values, within the experimental error.
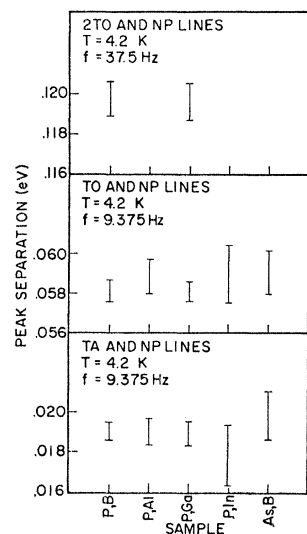
[15] G. G. Macfarlane, T. P. McLean, J. E. Quarrington, and V. Roberts, J. Phys. Chem. Solids 8, 388 (1959); Phys. Rev. 111, 1245 (1958).
[16] J. R. Haynes, M. Lax, and W. F. Flood, J. Phys. Chem. Solids 8, 392 (1959); 8, 422 (1959).
[17] J. R. Haynes, Phys. Rev. Letters 4, 361 (1960).
[18] B. N. Brockhouse, Phys. Rev. Letters 2, 256 (1959).

TABLE II. Spectral intensities and Coulomb energies corresponding to line peaks. $f=9.375$ Hz, $T=4.2$ K.

Silicon samples	Relative TO intensity ($\pm 30\%$)	$\dfrac{\text{NP intensity}}{\text{TO intensity}}$	E_{Coul}^{peak} (meV) NP line	E_{Coul}^{peak} (meV) TO line
(P,B)	1.000	0.22	17.2±0.2	17.2±0.5
(P,Al)	0.059	0.39	17.6±0.8	18.9±1.0
(P,Ga)	0.450	0.39	18.1±1.0	18.1±0.8
(P,In)	0.066	2.0	16.7±1.0	...
(Sb,B)	0.095	<0.03	...	18.6±0.9
(As,B)	0.042	0.42	18.5±1.0	20.0±1.0
(Bi,B)	0.030	0.49	...	21.4±1.0
(P,B)I	0.034	...	...	...
(P,B)II	0.028	0.21	...	...

The extra line appearing in the (P,In) spectrum at 0.943 eV (0.041±0.0015 eV below the energy of the NP peak) can be interpreted as a transition involving a photon and a longitudinal acoustical (LA) phonon with wave vector k_c. This assignment would lead to $k_c/k_{max}=0.76\pm0.06$, using the phonon dispersion curves of Brockhouse[18] and taking into account the estimated error in those curves of 3%. This is to be compared with a previous determination[19] of k_c/k_{max} based on an LA-phonon–assisted recombination which yielded 0.82, and with $k_c/k_{max}=0.85\pm0.03$ determined by the ENDOR technique.[20] The appearance of an LA-phonon–assisted transition is consistent with the work of Lax and Hopfield[21] which indicated that only the transition involving the longitudinal optical phonon was forbidden by symmetry. However, in most other optical emission and absorption experiments in silicon,[15–17] as well as in our results here for samples other than the (P,In) one, the LA-phonon–assisted transition is absent. This has not been satisfactorily explained. It should be noted in connection with disparities between

TABLE III. Impurity ionization energies and radii in silicon.

Impurity element	E_0 (eV) [a] Thermal	E_0 (eV) [a] Optical	Radii (nm) [b] a_1	Radii (nm) [b] a_2	Radii (nm) [b] r_1
Donors:					
P	0.044	0.045	2.11	0.93	
As	0.049	0.053	1.94	0.86	
Sb	0.039	0.043	2.16	0.95	
Bi	0.069	0.071[c]	1.69	0.74	
Acceptors:					
B	0.045	0.046			1.37
Al	0.057	0.067			1.12
Ga	0.065	0.071			1.11
In	0.16	0.154			0.75

[a] W. Kohn, Solid State Phys. 5, 257 (1957). See also R. L. Aggarwal and A. K. Ramdas, Phys. Rev. 140, A1246 (1965).
[b] A. Miller and E. Abrahams, Phys. Rev. 120, 745 (1960). The optical energies were used to calculate the radii.
[c] H. J. Hrostowski and R. H. Kaiser, J. Phys. Chem. Solids 4, 325 (1958).

[19] W. P. Dumke, Phys. Rev. 118, 938 (1960).
[20] G. Feher, J. Phys. Chem. Solids 8, 486 (1959); Phys. Rev. 114, 1219 (1959).
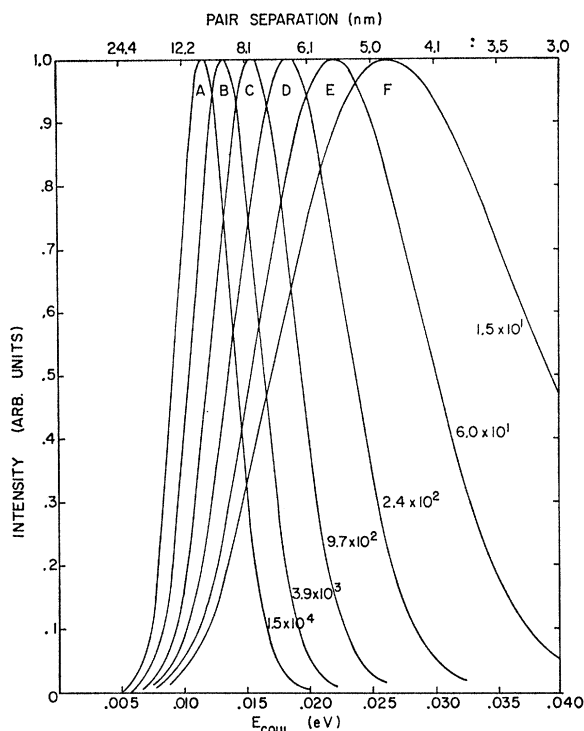[21] M. Lax and J. Hopfield, Phys. Rev. 124, 115 (1961).

FIG. 6. Theoretical spectral line shapes for the NP line, using anisotropic donor radii $a_1=2.11$ nm and $a_2=0.93$ nm. Values of the parameter W_0t are marked on the curves. The values of W_0t for the lines B, C, D, and E correspond approximately to the values found appropriate to the experimental curves at the four chopping rates used. Theory based on Refs. 4 and 14.

indium and other acceptors that indium has the largest ionization energy (0.154 eV) and would be expected to deviate most from conclusions based on an effective-mass formalism.

The ratios of the peak intensities of the NP and TO lines, which were only weakly dependent on chopping rate for all of our samples, are listed in Table II, together with the relative intensities of the TO lines in the various samples. As we go from a shallower to a deeper impurity of a given type (donor or acceptor), we would expect the bound carrier to have a greater spread in momentum space about the band extremum, thus favoring the NP process. This expectation of larger NP/TO intensity ratios for the deeper impurities is exhibited by the data, as seen in Table II. The most extreme manifestation of this dependence is the absence of the NP line in the (Sb,B) sample. However, even though Sb is indeed the weakest bound donor (see Table III), its ionization energy is so close to that of phosphorus that it is puzzling why the relative strength of the NP line in (Sb,B) is at least 10 times less than in (P,B). Other work on luminescence and absorption of excitons in silicon has exhibited similar behavior.[22]

[22] P. J. Dean, J. R. Haynes, and W. F. Flood, Phys. Rev. 161, 711 (1967); P. J. Dean, W. F. Flood, and G. Kaminsky, ibid. 163, 721 (1967).
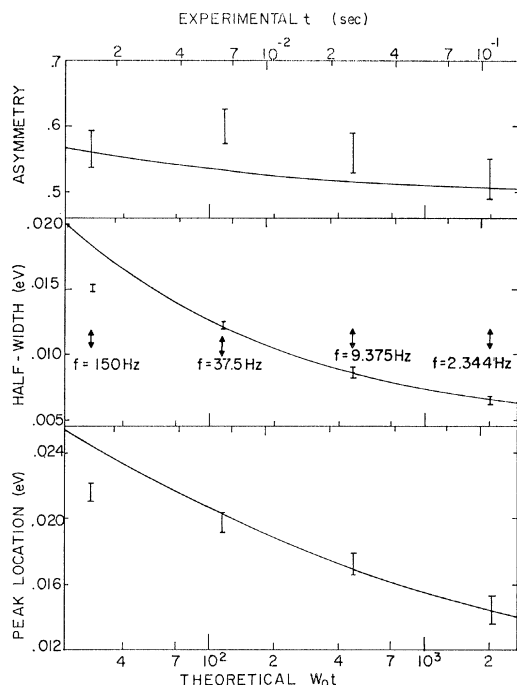
FIG. 7. Theoretical and experimental values of the peak location, half-width, and asymmetry for the (P,B) sample. Experimental values (shown as error bars) are referred to the time scale at the top of the graph, and theoretical values (shown as solid lines) are referred to the $W_0 t$ scale at the bottom of the graph. The theoretical calculations were for $a_1 = 2.11$ nm and $a_2 = 0.93$ nm. The peak location curve is derived from the theoretical curves of Fig. 6. The experimental peak locations are measured from an arbitrary zero.

The source of the TO intensity variation from sample to sample, as shown in Table II, is not well understood. It undoubtedly involves different clustering tendencies for the various impurities, as well as the variation in relative line intensities of the components of the spectrum. For a given pair of impurities, the intensity seems to depend predominantly on the acceptor concentration, over a wide variation of donor concentrations, as seen in Table II for the three (P,B) samples used. This is suggestive of a form of donor clustering about acceptors.

The small difference in linewidth between the NP line and its phonon-assisted replicas is probably due to the energy spread of the participating phonon, rather than to a difference in Coulomb broadening between the two types of lines, since the results of Sec. 4 B suggest comparable Coulomb energies of pairs responsible for the NP line and for the phonon replicas.

B. Determination of E_{Coul} and W_0

From Eq. (1) it is seen that E_g can be determined if the pair separation (and thus the value of E_{Coul}) that predominantly contributes to some part of the experimental curve can be found. This is because E_A, E_D, and E_{phonon} are known, and E_{photon} is just the experi-

mental photon energy at the point in question. Such a determination of E_g is independent of the value of the exciton binding energy E_{exc}, in contrast to previous work,[15,23] where E_g was determined by adding the estimated exciton binding energy to an accurately measured absorption threshold energy or recombination energy. We shall work with the value of E_{Coul}^{peak}, corresponding to the peak of the experimental curve, and therefore rewrite Eq. (1) to correspond to this choice

$$E_g = E_{photon}^{peak} + (E_A + E_D) + E_{phonon} - E_{Coul}^{peak}. \quad (12)$$

Here E_{photon}^{peak} corresponds to the photon energy at the peak of the experimental line. Of course, the sum of the impurity ionization energies could be determined from Eq. (12) if E_g were taken as known.

In order to determine E_{Coul}^{peak} and W_0, $I(E,t)$ was computed from Eq. (11) for various values of the donor radii a_1 and a_2, using $W_0 t$ as a parameter, since W_0 and t enter into the line shape only in the form of their product. These calculations were performed on a digital computer, which was programmed to modify the results by including the effect of the finite spectrometer bandpass. The curves were then normalized to unity in order to facilitate comparison with experiment. A result of this calculation is plotted in Fig. 6, where $a_1 = 2.11$ nm and $a_2 = 0.93$ nm, the values appropriate to a phosphorus donor (see Table III). The values of $W_0 t$ increase by factors of 4 as we progress from curve to curve toward higher energies. For a given W_0, this corresponds to changes of a factor of 4 in delay time or, equivalently, in chopping rate. If the theory is applicable to this experiment, it should be possible to superimpose the theoretical curves and the set of normalized experimental curves for the various chopping rates. Comparison of Fig. 6 with Fig. 4 illustrates the excellent correspondence. E_{Coul}^{peak} is then equal to the energy at the peak of the matched theoretical curve, since the theoretical zero of energy was taken at $E_g - (E_A + E_D) - E_{phonon}$, and W_0 is found by comparing $W_0 t$ and t for matched theoretical and experimental curves.

This analysis assumes that the predominant contribution to the linewidth comes from the Coulomb interaction. Infrared-absorption studies of the transitions from impurity ground states to excited states have shown that the ground states have widths less than or on the order of 0.5 meV,[24,25] which is to be compared with the narrowest lines that we observed, at $f = 2.344$ Hz, of 6 meV. This comparison supports our assumption. NP and phonon-assisted lines likewise have width differences of less than 1 meV, suggesting that the width contribution due to phonon energy spread may also be neglected.

[23] J. R. Haynes, M. Lax, and W. F. Flood, in *Proceedings of the International Conference on Semiconductor Physics, Prague, 1960* (Academic Press Inc., New York, 1961), p. 423.
[24] J. J. White, Can. J. Phys. **45**, 2797 (1967).
[25] J. W. Bichard and J. C. Giles, Can. J. Phys. **40**, 1480 (1962).

The application of the above method is strictly applicable only to the NP line, since the theoretical equation (4) was derived only for this case. However, it is reasonable to believe that the exponential dependence of $W(R)$ is the same for the phonon-assisted transitions as for the NP transitions. In this case, the analysis will yield a good value for E_{Coul} of the phonon replicas, but the W_0 of the phonon-assisted transitions must be treated as a phenomenological rate constant, not necessarily related to the W_0 of Eq. (4).

In order to facilitate curve matching, the three parameters of peak position, half-width, and asymmetry (fraction of the half-width above the peak energy) were chosen to determine best fits between theory and experiment. Typical examples of these comparisons are shown in Fig. 7, where the theoretical curves and experimental points are shown superimposed. To effect the match of half-width and asymmetry, the theoretical curves are displaced horizontally relative to the sets of experimental points until the best fit is obtained. The horizontal displacements must, of course, be identical for each parameter so as to keep the relationship between t and W_0t the same for each. For matching the peak locations, relative vertical displacements are also permitted, since only the rate of change of peak location with t, or the slope of the peak energy versus t curve, must be matched.

The agreement between theory and experiment is quite good, with the exception of the points corresponding to $f = 150$ Hz. These were ignored during curve fitting because of the lack of saturation at that chopping rate. The asymmetry is sensitive to relatively small variations in the location of the high-energy half-intensity point which corresponds, for the 37.5-Hz curve, to the 50-Å impurity-separation limit, below which the theory begins to break down (see Fig. 6). This may explain the discrepancy in theoretical and
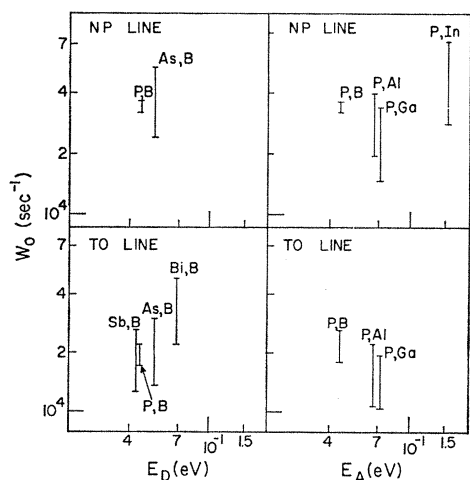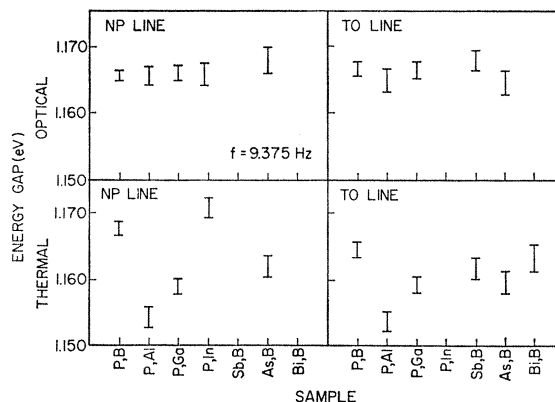

FIG. 9. Calculated energy gap using optically and thermally measured impurity ionization energies. Chopping rate=9.375 Hz, $T = 4.2$ K.

experimental asymmetry in Fig. 7. Similar results were obtained for the other samples when the appropriate donor radii were used in the computation, although the errors were greater since the experimental errors were appreciably larger with these samples. In order to test the hypothesis that the donor and acceptor radii enter asymmetrically in this calculation, we repeated the above analysis using the acceptor radius r_1 in place of the smaller donor radius a_2 in those cases where r_1 was appreciably greater than a_2 [for example, (P,B)]. The major change was a decrease of about 5 or 6% in the value of the theoretical asymmetry over the range in which our comparisons were made. This makes the agreement bad at all frequencies and favors our former treatment. For comparison, we also investigated the case of spherical donors with radii ranging from 1.4 to 2.1 nm, and similar lack of agreement, with asymmetries less than 0.5, was obtained. Because of the better agreement between theory and experiment, we used the anisotropic a_1 and a_2 values from Table III in our calculations.

The values determined for E_{Coul}^{peak} and for W_0, for both the NP and TO lines at 9.375-Hz chopping rate, are shown in the last column of Table II and in Fig. 8, respectively. A comparison of the theoretical and experimental magnitude and functional form of W_0 with the results on the NP line can now be attempted. From Eq. (4) and the approximate proportionality[26] of the shallow-impurity Bohr radius to the square of the ionization energy, one predicts $W_0 \propto E_A^{5/2}E_D^{3/2}$. The results in Fig. 8 are not sufficiently precise to test this prediction, although, within the experimental error, they are compatible with it. From Eq. (4) the magnitude of W_0 is calculated to be 5×10^1 sec^{-1}, while the experimental value is approximately 3×10^4 sec^{-1}. The origin of this discrepancy of almost three orders of magnitude is not clear at present.

Using the measured values of W_0, the peak values of $I(E,t)$ were calculated as a function of chopping rate

FIG. 8. Experimental W_0 versus impurity ionization energies E_A and E_D for various combinations of donors and acceptors. $T = 4.2$ K, chopping rate = 9.375 Hz.

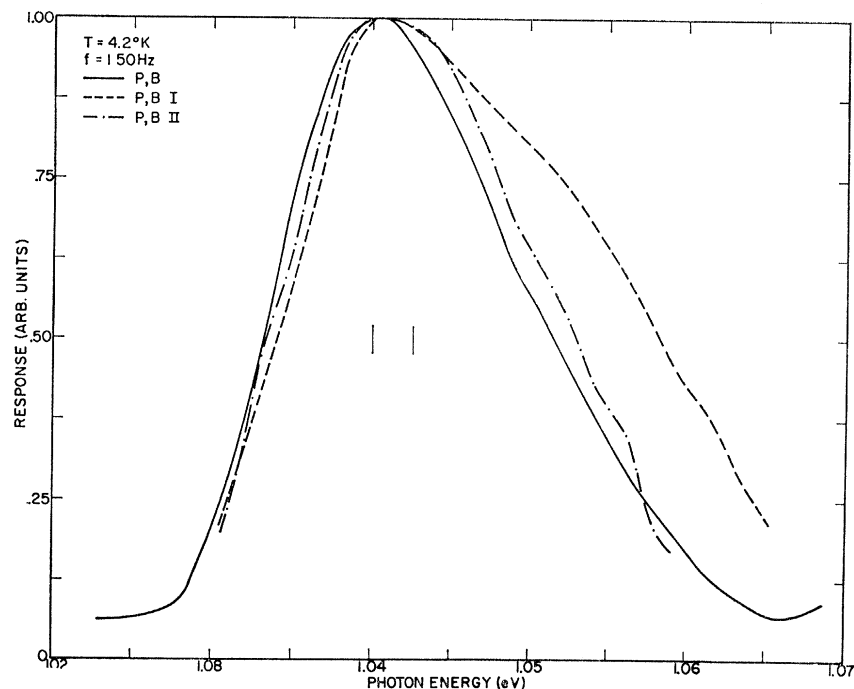[26] A. Miller and E. Abrahams, Phys. Rev. 120, 257 (1957).

FIG. 10. Luminescence spectra of silicon samples as a function of impurity concentration at 150-Hz chopping rate. Donor concentrations: (P,B), 6×10^{16} cm^{-3}; (P,B)I, 6×10^{15} cm^{-3}; and (P,B)II, 1.8 $\times10^{17}$ cm^{-3}. $T=4.2$ K.

and compared with the experimental TO peak intensities. A normalized representative comparison at four different chopping rates for the (P,Ga) sample is as follows:

f (Hz)	Intensity (calc)	Intensity (expt)
150	4.0	1.9
37.5	2.2	1.6
9.375	1.00	1.00
2.344	0.35	0.5

Comparable results were obtained with other impurity combinations. Neglecting the $f=150$-Hz results, since the experimental results there are bound to be low because of nonsaturation, the agreement is satisfactory. It is possible that donor clustering about the acceptor can account for the deviations.

C. Energy Gap, Exciton Binding Energy, and Impurity Binding Energies

E_g was calculated for the various samples using Eq. (12) and the values of $E_{\mathrm{Coul}}{}^{\mathrm{peak}}$ listed in Table II. Thermally and optically determined impurity ionization energies, listed in Table III, were utilized. Both sets of results are plotted in Fig. 9. It is seen that the optically determined ionization energies lead to a consistent value of 1.166 ± 0.001 eV for E_g (4.2 K), whereas the thermal energies give values of E_g determined from the different samples which differ by amounts exceeding the experimental error. This gives strong support for the thesis that the optical ionization energies are the correct ones for the majority of the individual impurities, and that the thermally measured activation energies are due to complicated processes such as

carrier redistribution, cluster formation, and Coulomb interaction with charged impurities. Using the value of E_g derived with the aid of the optically measured ionization energies and combining this with the value $E_g(4.2\text{ K})-E_{\mathrm{exc}}=1.1558$ eV, as determined by optical-absorption techniques,[15] where E_{exc} is the exciton binding energy, one obtains $E_{\mathrm{exc}}=0.0102\pm0.0015$ eV. An early theoretical treatment[27] of the exciton yielded an order of magnitude estimate of 10 meV for the exciton binding energy, and an estimate of E_{exc} based upon an experimental fit to a simple hydrogenic model[15] gave a value 7–10 meV. An estimate of E_{exc} from a recombination-radiation experiment[23] resulted in a value of 8 meV. More recent theoretical work[28,29] predicts an exciton binding energy of 0.012–0.014 eV.

D. Temperature and Concentration Dependence

The temperature dependence of the recombination spectrum in the (P,B) sample was investigated between 4.2 and 1.03 K but no significant change in either the intensity or the shape of the spectrum was observed. Preliminary measurements were also made at 20 K and a 150-Hz chopping rate on this sample. The most striking effect here was the reduction of the linewidths by a factor of almost 2 relative to the 4.2-K linewidth. The lines also became symmetrical, shifted towards low energy by about 0.002 eV, and increased in amplitude by approximately a factor of 2.

[27] G. Dresselhaus, J. Phys. Chem. Solids 1, 14 (1956).
[28] T. P. McLean and R. Loudon, J. Phys. Chem. Solids 13, 1 (1960).
[29] T. P. McLean, Progr. Semicond. 5, 53 (1960).

The effects seen at 20 K are most likely due to electron impurity hopping and carrier redistribution among the impurities prior to recombination. The lack of temperature dependence in the liquid-helium-temperature range indicates that hopping has a negligible influence on radiative recombination at times shorter than or about equal to 10^{-1} sec and need not be included in the theory.

The concentration dependence of the TO lines for three (P,B) samples at $f = 150$ Hz is shown in Fig. 10. The significant difference among these curves is the broadening on the high-energy side of the line for the dilute sample. The other differences are within the noise due to the small signals from the most dilute and most concentrated samples. At 9.375 Hz, the differences among the lines become barely discernable. The high-energy side broadening of the dilute sample at short times is expected, since we have a smaller number of ionized impurities competing for the same number of free carriers. This means that a greater percentage of the close pairs will be neutralized and the sample will be more saturated at short times. The lack of any other concentration dependence in the line shape is in accord with the theory, and supports the contention that thermal ionization energies are due to statistical effects and charge redistribution, rather than to actual change of ionization energy of the majority of neutral impurities, since previous work indicated a large change of thermal activation energy with impurity concentration.[30],[31] In particular, a decrease in thermal activation energy of about 8 meV relative to a very dilute sample was reported for an impurity concentration of $10^{17}/$ cm^3, whereas our results for sample (P,B)II [$N_D = (1.8 \times 10^{17})/$cm^3] shown in Fig. 10 indicate that any energy shift relative to the dilute sample occuring in our measurements is at least an order of magnitude smaller than the reported thermal activation energy shift.

Thus, it is strongly suggested by the concentration-dependent studies and by the inapplicability of the thermal ionization energies to the determination of the energy gap, that thermal-activation experiments are sensitive mainly to shallower energy states, provided that there is a mechanism for efficiently transferring carriers from the deeper states to the shallower ones. An appreciable change in activation energy may thus easily result from a relatively small number of impurity complexes, which have a decreased ionization energy, together with an efficient hopping or tunneling process which allows carriers from other impurities to migrate to the complexes.

A more complete investigation of temperature and concentration effects on linewidths and radiation intensities is now in progress.[32]

5. SUMMARY

Radiative electron transfer from shallow donors to shallow acceptors in silicon has been observed with an NP component, as well as TO- and TA-phonon-assisted components, in partial agreement with the selection rules of Lax and Hopfield. In addition, a (P,In) sample exhibits an LA-phonon-assisted component. Other deviations in relative intensities of the component lines, related to phonon selection rules, are also reported.

Using anisotropic wave functions in the analysis of the line shape at different delay times after neutralization of impurities, good agreement with experiment was obtained. The width of the indirect energy gap was determined independently of the exciton binding energy. Combining the gap measurement with infrared-absorption measurements near the indirect transition threshold yielded a value of the exciton binding energy.

The impurity ionization energies were found to be consistent with the optically measured values but not with the thermally measured ones. In connection with this, no change in ionization energies was seen up to donor concentrations of $(1.8 \times 10^{17})/$cm^3. The thermal activation energy changes with concentration are attributed to carrier redistribution effects, clusters, and Coulomb interactions with charged acceptors.

ACKNOWLEDGMENTS

[30] J. F. Barnes and R. H. Tredgold, Proc. Phys. Soc. (London) **78**, 716 (1961).
[31] R. S. Levitt, Bull. Am. Phys. Soc. **7**, 89 (1962).
[32] J. G. Constantine and A. Honig, Bull. Am. Phys. Soc. **13**, 727 (1968).